JCTC Journal of Chemical Theory and Computation

Article

pubs.acs.org/JCTC

Cooperativity Assisted Shortening of Hydrogen Bonds in Crystalline Oxalic Acid Dihydrate: DFT and NBO Model Studies

Jernej Stare* and Dušan Hadži

National Institute of Chemistry, Hajdrihova 19, 1000 Ljubljana, Slovenia

Supporting Information

ABSTRACT: The distance of ∼2.49 Å separating the carboxylic OH oxygen from the water oxygen atom in the α-polymorph of crystalline oxalic acid dihydrate is by ∼0.1 Å shorter than the average distance in carboxylic acid monohydrates. It is also by ∼0.2 Å shorter than the corresponding distance presently calculated for the heterotrimer consisting of one acid and two water molecules. The large difference between $R_{O\cdots O}$ in the heterotrimer and in the crystal is attributed to the cooperative effect in the latter; this is supported by calculations carried out on clusters constituted of an increasing number of acid and water molecules. The present DFT calculations with geometry optimization include seven isolated model clusters, the largest of which contains five acid and eight water molecules. The $R_{O\cdots O}$ of the short hydrogen bond shortens progressively with increasing the number of cluster constituents; in the largest cluster, it reaches 2.50 Å. This is remarkably close to both the experimental distance as well as to the distance obtained by the periodic DFT calculation. The electronic effects were studied by Natural Bond Orbital analysis, revealing an enhancement of hydrogen bonding on extending the network by increased polarization of the carbonyl group and by the increased delocalization interaction between the lone electron pair on the acceptor oxygen atom and the OH antibond orbital. The formation of circular motifs appears to be the most important factor in the cooperative shortening of the hydrogen bonds. In agreement with the measured hydrogen bond distances, inspection of the electron density reveals a notable difference in hydrogen bond shrinking tendency between the two known polymorphs of the title system.

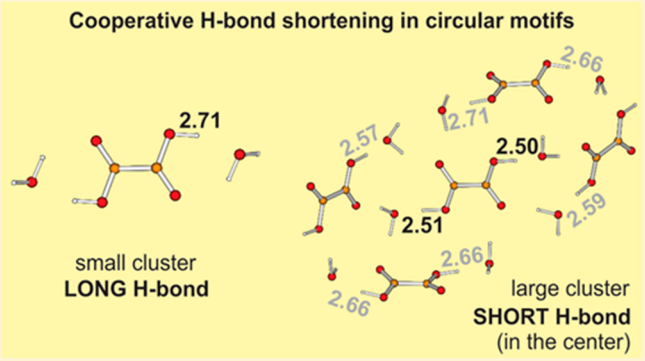

1. INTRODUCTION

Oxalic acid dihydrate (OADH) in the crystalline solid state represents an interesting species that, albeit known since 1920s, is still producing many surprises. The crystal structure of its α-polymorph (α-OADH) has been the object of numerous X-ray diffraction (XRD) studies after the first publication in 1936.[1] The early results were corrected by Robertson and Ubbelohde who also investigated some other physical properties of α-OADH.[2] Several studies were done in the following decades, including XRD measurements at higher accuracy,[3] alternative models and improved refinement,[4,5] isotope effects,[6,7] neutron diffraction structure determination,[8−11] and high resolution electron density studies.[12−14] A series of results was obtained within the project organized by the International Union of Crystallography.[15] This exercise was primarily focused on the electron density and its deformation caused by the hydrogen bonding (H-bonding) but has also yielded improved structural data,[16] including temperature effects.[17] Further on, α-OADH was subject to improved charge density studies at low temperature.[18,19] The most recent XRD study presented the high pressure effects; the bond metric results obtained at normal pressure are in good agreement with earlier work.[20] Recently, α-OADH was used as benchmark for the new single crystal neutron diffractometer at the Oak Ridge National Laboratory.[21] A corollary to the experimental work was the theoretical treatment of the electron density focused on the H-bonding,[22−25] particularly by the short H-bond ($R_{O\cdots O} \approx 2.49$ Å) connecting the acid's OH group to the water oxygen (SHB henceforth). This and the longer H-bonds ($R_{O\cdots O} \approx 2.83$ Å) formed between the accepting carbonyl group and the two donating water molecules (LHB henceforth) form a three-dimensional network consisting of quasi-circular motifs of acid molecules connected by the SHBs with water molecules that are lying approximately in the plane of the acid. The planes are connected by longer H-bonds with water molecules as donors. These motifs with interlayer connections may also be considered as spirals.[2] Very similar structures were also found with the acetylene dicarboxylic and diacetlyene dicarboxylic acid dihydrates.[26,27] However, $R_{O\cdots O}$ in these crystals is slightly (by up to 0.05 Å) longer.

OADH exhibits polymorphism. The beta form (β-OADH) crystallizes only from deuterated solutions and features very similar packing features as α-OADH, having topologically almost the same motif within the first coordination sphere. However, the torsional alignment of molecules is slightly different and apparently less favorable for the formation of short H-bond;

Received: December 6, 2013
Published: March 13, 2014

   dx.doi.org/10.1021/ct500167n | J. Chem. Theory Comput. 2014, 10, 1817−1823

$R_{O\cdots O}$ of the SHB in deuterated β-OADH amounts to 2.54 Å,[28] as compared to 2.49 Å in deuterated α-OADH.[11] Unlike α-OADH, which has evolved into a benchmark system for crystallographic techniques, the β-polymorph is less common and has been subject of fewer investigations. Recently, the high pressure effect on H-bond of both polymorphs was studied by neutron diffraction supported by periodic DFT calculations, yielding evidence that the pressure-driven proton migration in the SHB is less favorable in the β-polymorph.[29]

The SHB in α- and β-OADH is on the short side of the group of carboxylic acid monohydrates collected by Steiner.[30] The author calculated the average of the group to be 2.591 Å. A later search carried out by Vishweshwar et al. yielded some examples of such acid hydrates with $R_{O\cdots O} < 2.50$ Å.[31] Recently, these authors have added a series of pyrazine di-, tri- and tetracarboxylic acid hydrates with $R_{O\cdots O}$ between 2.47 and 2.55 Å.[32] The study is focused on the synthon interesting for crystal engineering; the concept of synthon-assisted H-bonding was proposed as an addition to the already established categories of resonance-, charge-, and polarization-assisted H-bonding.[33] The shortness of the acid-to-water H-bonding was attributed to the cooperative effect supported by the polarization of the C═O groups owing to accepting of two H-bonds from the two water molecules. However, this was not supported by a quantitative theoretical model. α-OADH was also included as an example, because it features a bent-chain motif of H-bonding common to the series.

Vishweshwar et al. were the first to point out the shortness of SHB in α-OADH and related systems. Interestingly, despite numerous earlier studies on the crystal structure of α-OADH, no particular attention was paid to the shortness nor were its origins examined by experimental and theoretical treatments. In addition, not much information is available about the H-bonds between oxalic acid and water either in the gas phase or in solution. The intriguing fact motivating the present research is that the entry level calculations in the gas phase and in the continuum solvation model fail to reproduce the observed shortness of the SHB in α-OADH, underestimating $R_{O\cdots O}$ by ~0.2 Å. This is in agreement with the experimental evidence on oxalic acid in polar solution suggesting that the H-bond is of rather modest length and strength. For instance, the infrared spectrum of aqueous solution of oxalic acid exhibits a broad and strong absorption culminating at about 2900 cm^{-1} and assigned as the OH stretching mode (see Supporting Information, Figure S1a) that corresponds roughly to $R_{O\cdots O} \approx 2.65$ Å, as in carboxylic acid dimers or chains.[34,35] Similarly, the OH stretching mode of the crystalline anhydrous oxalic acid appears at about 3000 cm^{-1} (Supporting Information, Figure S1b), corresponding to the measured O···O distance of 2.67−2.70 Å.[36] In contrast, the OH stretching band in the crystalline α-OADH is very complex and covered by other vibrations. However, from the Raman and infrared spectra[37] the band can be estimated to reach its maximum at about 1900 cm^{-1} (Supporting Information, Figure S1c), which corresponds well to the shortness of the SHB. The shortness also cannot be based on proton donating and accepting properties of the involved species, considering the difference in pK_a values of the acid and hydronium ion which equal 1.23 and −1.74, respectively.

The shortening of $R_{O\cdots O}$ in crystalline α-OADH is obviously caused by a crystal effect and cooperativity is the most probable reason for it. Cooperativity was evoked already by Robertson and Ubbelohde[2] and, more recently, by Visweshwar et al. in their study of synthons.[31,32] Three motifs for cooperation appear to be possible in the example of α-OADH: spiral, chain, and quasi-circular, all consisting of alternating acid and water molecules that act both as H-bond donors and acceptors. A theoretical model appears necessary to support the engagement of cooperativity along the possible motifs. The existing theoretical studies of cooperativity within H-bonded chains include hydrogen cyanide,[38,39] as well as chains of formamide. The latter have been proposed as models of cooperative effects in protein folding,[40,41] optionally with some other small molecules such as water and urea.[42] Cooperativity within circular motifs has been studied in rings formed by water molecules treated at various levels of theory,[43] as well as for the cyclic complexes of formamide, hydrogen fluoride and hydrogen cyanide.[44,45] A recent study of cooperativity in hydrogen cyanide clusters considers both chain and circular motifs and puts emphasis on dipole-polarizability.[46] Most of the calculations deal with cooperation along chains or circular structures, but less with three-dimensional aggregates. An example of the latter is the study of H-bonds in water clusters exhibiting cooperative effect.[47] Cooperativity within H-bond networks appears to contribute to the stability of polypeptide β-sheets, as demonstrated for polyglutamine by DFT and QM/MM calculations.[48]

The focal point of the present study is the theoretical treatment related to the origin of shortness of the SHB in OADH. A theoretical modeling approach to the H-bonding in OADH appears interesting not only because of the shortness of the SHB but also for other H-bond-based physical properties of crystals that have already been studied with OADH, including polaron based electrical conductivity,[49] nuclear magnetic resonance,[50,51] nuclear quadrupole coupling,[52] and vibrational spectroscopic characteristics.[37,53] Theoretical studies related to these characteristics did not pay particular attention to the shortness of SHB. The present approach to the cooperativity in OADH is based on the evolution of metric parameters, the trends in atomic charges and bond-antibond stabilization energies with increasing agglomeration of the acid and water molecules. The difference between the α and β polymorphs associated with the alignment of molecules and its impact of on the H-bond shortening is also examined.

2. METHODS AND MODELS

2.1. Optimized Isolated Clusters. The clusters studied in this work are shown in Figure 1a−g; they are labeled according to the number of acid and water molecules, for example, 1A2W denotes one oxalic acid molecule accompanied by two water molecules bonded to each of the acid hydroxyl groups; this is the smallest cluster considered in the present study (Figure 1a). This cluster was expanded by adding another water molecule to each of the carbonyl groups forming LHB (1A4W, Figure 1b) and further on by connecting two acids by two water molecules (2A2W) thus forming a ring of two SHBs and two LHBs (Figure 1c). The clusters were gradually expanded by adding acid and water molecules in cyclic arrangements. The series was completed with the 5A8W cluster (Figure 1f). These clusters were treated as isolated systems except for 1A2W that was also subject to the continuum solvent reaction field of a medium of high polarity (ε = 36 and ε = 80, corresponding to acetonitrile and water, respectively).[54] Geometry optimization of the clusters was performed at the BLYP/6-31+G(d,p) level of theory by the *Gaussian 09* program package[55] trying to keep their point group symmetry during optimization, but without enforcing any other geometric constraints or restraints. Default force and displace-

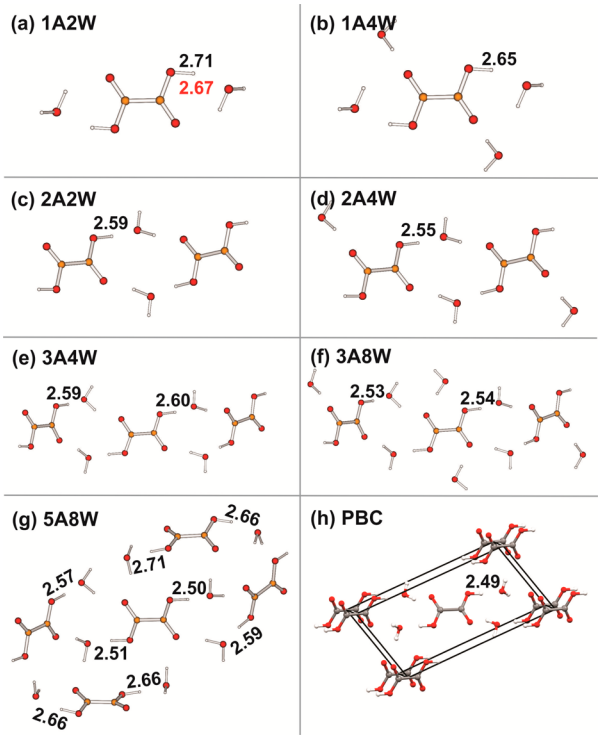

Figure 1. (a–g) BLYP/6-31+G(d,p) optimized structures of the oxalic acid and water clusters with the O···O distances of the acid-to water hydrogen bond (SHB); (h) unit cell of the periodic model with the BLYP/PW optimized O···O distance of SHB. The value in part a displayed in red corresponds to the calculation under the polar solvent reaction field.

ment convergence criteria were used. The modest basis set is known to be adequate for calculations on H-bonds and particularly so when considering a series of chemically related systems.

2.2. Periodic Models. The periodic model of α-OADH (Figure 1g) and β-OADH (not shown) utilized the plane wave methodology coupled with the BLYP density functional, as implemented in the CPMD v. 3.13.2 program.[56] The plane wave cutoff was set to 80 Ry and the core electrons were approximated by atomic pseudopotentials of Troullier and Martins.[57] A $2 \times 4 \times 1$ and $2 \times 4 \times 4$ Monkhorst-Pack mesh of k-points[58] was used in the electron structure calculations for α-OADH and β-OADH, respectively. Optimization of the atomic positions was performed under the constraints of the $P2_1/n$ and $P2_1/a$ space group for α-OADH and β-OADH, respectively, and by fully considering periodic boundary conditions (PBC). The unit cell parameters and the initial atomic positions were taken from the crystallographic data of Martin and Pinkerton for α-OADH,[19] and of Iwasaki and Saito for β-OADH.[28] The unit cell parameters were kept fixed during optimization.

In order to validate the BLYP methodology employed in our calculations, we performed optimization of the selected clusters and of the periodic models by using the PBE and B3LYP functionals, following the same procedure as described above. Additional details on these calculations are given in Supporting Information (section S2).

2.3. Electron Density Analysis (NBO). The BLYP/6-31+G(d,p) electron density study of selected model clusters related to ring formation and cooperativity (Figure 2) was performed by the Natural Bond Orbital (NBO) analysis methodology (v. 3),[59] as implemented in the *Gaussian 09* package, yielding atomic charges and bond-antibond stabilization energies. Details on the construction of models are given in section 3.2. The total interaction energy of the clusters (relative to its molecular constituents) was computed at the same level of theory and counterpoise-corrected for the basis set superposition error. In the same way as above, NBO calculations were also applied to model clusters used in the comparison between α- and β-OADH (section 3.3). The location of electron lone pairs involved in the comparison was computed by the Wannier localization method[60,61] included in the CPMD v. 3.13.2 program.

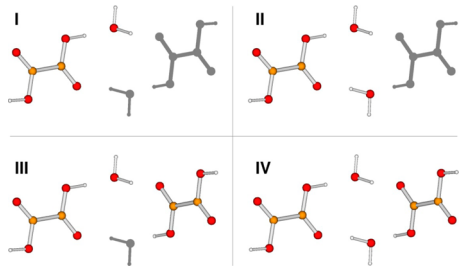

Figure 2. Models for the NBO analysis of the influence of intermolecular interactions on the short hydrogen bond between oxalic acid and water. Molecules not included in the calculation are shown in gray.

3. RESULTS AND DISCUSSION

3.1. Geometry Optimization of the Cluster and Periodic Models. The first treated example is the 1A2W cluster (Figure 1a). Its $R_{O\cdots O}$ of 2.71 Å is by ~0.2 Å longer than the experimental value. Application of SCRF with $\varepsilon = 36$ or $\varepsilon = 80$ shortens it by only 0.04 Å. A slightly superior effect is produced by adding two more water molecules bound to the C═O groups as in the 1A4W cluster (Figure 1b). This results in the shrinking of $R_{O\cdots O}$ to 2.65 Å. Significant shortening of SHB occurs with the formation of a circular structure from two acid and two water molecules (2A2W, Figure 1c; $R_{O\cdots O} = 2.59$ Å), and on adding two water molecules to the vacant C═O groups the O···O distance shrinks even further, that is, 2.55 Å (2A4W, Figure 1d). The expansion of clusters 2A2W and 2A4W by adding another acid and water couple, forming double ring clusters 3A4W and 3A8W (Figure 1e,f), does not result in a notable change of $R_{O\cdots O}$. However, the minimal $R_{O\cdots O}$ is reached in the two central SHB's of the largest cluster 5A8W (Figure 1g); the distances of 2.50 and 2.51 Å are almost identical to the diffraction results. The fully periodic approach also yields a remarkable agreement with the experimental SHB length. The calculated value of 2.49 Å is within the fluctuations of $R_{O\cdots O}$ measured by different authors (e.g., refs 9–13). Clearly, the agreement is not limited to the SHB and LHB geometries and the periodic calculation reproduces correctly the other structural parameters as well.

The shortening of the LHB is less dramatic than with the SHB. In the 1A4W cluster (Figure 1b) the $R_{O\cdots O}$ of LHB is 2.96 Å while in the 5A8W cluster the LHB lengths vary between 2.77 and 2.90 Å. However, due to the limitations of the models originating in their large torsional flexibility, the accuracy of the calculated LHB lengths is somewhat limited (see below).

The comparison of the model clusters suggests that ring formation is probably the most efficient factor for the shortness of SHB in the present system. The formation of rings with alternating acid and water molecules contributes notably to the

dx.doi.org/10.1021/ct500167n | J. Chem. Theory Comput. 2014, 10, 1817–1823

shrinkage of $R_{O\cdots O}$. However, the overall agglomeration around a selected oxalic acid molecule seems to be also very important for the shrinking of $R_{O\cdots O}$, for instance, the SHB in the center of the 5A8W cluster is shorter than in the 3A4W or 3A8W clusters. Despite the better agreement with the experiment, the periodic calculation with fully featured symmetry does not provide any significant improvement of the SHB length relative to the 5A8W cluster model. However, the difference in $R_{O\cdots O}$ between the 2A2W and the periodic model (the latter yielding by ∼0.1 Å shorter distance) indicates that at least part of the shortening is caused by the crystal field and not only by cooperation within the circular motifs. A notable feature of both the 5A8W cluster and the crystal is the H-bonding of two water molecules to the acid's carbonyl groups.[32] Such bonding corresponds to the conditions for effective cooperation deduced by Del Bene and Pople from their study of clusters of water molecules.[43]

An arguable shortcoming of the nonperiodic 5A8W model cluster is the offset of certain structural parameters from the experimental structure. This is particularly serious with the torsional degrees of freedom. Owing to the absence of geometric restraints which are otherwise enforced by the crystal field, the torsional angles between the molecules are not comparable with those found in the crystal and the H-bonded network in the cluster is not identical to one in the real structure. Despite of the attempts at following the point group symmetry during optimization, the two SHB distances formed by the central oxalic acid molecule (Figure 1g) are not equal. It should be noted that the apparent proximity between the two adjacent water molecules in the top center of the 5A8W cluster (Figure 1g) is an artifact of the projection. Remarkably, the absence of planarity of the circular motifs in both the cluster and in the crystal structure does not impede the shortening of the SHB.

Another difficulty of the cluster models is the fact that the substantial torsional flexibility of the intermolecular potentials permits numerous configurations of the water molecules around the oxalic acid molecule. Particularly if the model includes a relatively large number of weakly bonded water molecules (e.g., in the 3A8W cluster, Figure 1f), the variations in the optimized structures such as the tendency of forming H-bonds between water molecules or H-bond donation to the carboxylic C−O−H oxygen atom and similar faults occur. For instance, a rather unexpected result was obtained in the attempt at optimizing the cluster consisting of one acid and six water molecules with two of them bonded to each of the carbonyl groups. The starting metric parameters corresponding to the crystal metrics changed soon to a structure in which one water molecule lost the contact with the carbonyl group and established a weak H-bond to the hydroxylic oxygen of the acid, acting as a donor. The limited stability of the arrangements taken from the crystal structure and treated as an isolated cluster is a clear indication that such arrangements are stable only under the conditions present in the crystal. Consequently, the corresponding O···O distances may differ slightly from the values displayed in Figure 1. However, variations in the SHB due to torsional flexibility and water rearrangements are small (up to 0.03 Å), and the general trend of shortening on agglomeration is sustained. Variations in LHB are larger; usually the O···O distances are in the range between 2.75 and 2.95 Å, but the trend of shortening on agglomeration is still evident. For instance, the LHB in the 1A4W cluster (Figure 1b) amounts to 2.96 Å, but when participating in the ring as, for instance, in the 2A2W cluster (Figure 1c) it shrinks to 2.75 Å.

3.2. NBO Electron Structure Analysis. The clusters subject to the NBO analysis are displayed in Figure 2. In order to achieve the clearest expression of the electronic effects acting in cooperativity and to ensure maximum comparability between the results the internal geometry parameters were kept fixed in all models; hence, the difference in the properties of the density originates solely from the electron effects but not from changes in internal geometry parameters such as bond lengths, valence angles, or torsional angles. The models were built on the basis of the cluster shown in Figure 2 IV obtained by partial geometry optimization in which the SHB was fixed to 2.70 Å while the LHB was fixed to 2.80 Å. The value of 2.70 Å corresponds roughly to the fully optimized 1A2W cluster (Figure 1a) while the value of 2.80 Å is close to the experimentally determined lengths of LHB. From model IV, one individual water and/or acid molecule was removed in order to obtain the smaller models (I−III). Model I is the simplest of the four, containing only the interacting acid and water. Model II has an additional water molecule bound to the C═O group of the acid. Model III is derived from model I by expanding it with an additional acid molecule accepting a hydrogen bond from the water molecule at the C═O group. Model IV combines both expansions of model II and III, resulting in ring formation.

The NBO analysis of the electron density was performed and the characteristic quantities such as atomic charges and bond−antibond stabilization energies of the cluster models were examined. The analysis is focused on the O_1—H···O_2 moiety of SHB and its sensitivity to the environment in which it is embedded (for atom labels see Figure 3). The influence of the

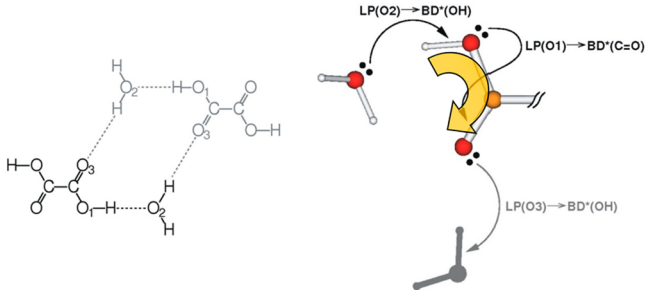

Figure 3. Left: schematic representation and atom labeling of the oxalic acid dihydrate model accompanied by optional water molecules bound to the C═O groups (shaded). Right: hydrogen bond moiety with donor−acceptor interactions between lone pair and antibond orbitals. The yellow arrow indicates the shift in electron density resulting from hydrogen bonding.

following factors was investigated: (i) the effect of the water molecule forming a LHB with the C═O_3 group of the acid, (ii) participation of the SHB-accepting water molecule in the LHB as a H-bond donor to the C═O_3 group of another acid molecule, and (iii) the formation of ring clusters with alternating acid and water molecules, which is, in essence, a cooperative combination of (i) and (ii). Selected characteristic quantities obtained by the NBO analysis of the density are listed in Table 1. A schematic representation of the structure and electronic effects is presented in Figure 3.

Consistent trends in natural atomic charges characterizing the models are notable although some of the changes are small. Addition of a water molecule to the C═O_3 group (model II) enhances the polarization of the C═O_3 bond. On the contrary, addition of another acid molecule (model III) results in a minor additional polarization of the C═O_3 bond. Combining both interactions thus closing the ring (model IV) results in a

Table 1. Selected Atomic Charges, Composition of the Oxygen Contribution to the OH Bond Orbital, Donor−Acceptor Stabilization Energies between the Oxygen Atom Lone Pair and the Selected Vacant Antibond Orbitals,[a] and the Total Interaction Energy Computed As Energy Difference between the Entire Model and the Individual Molecules

	model I	model II	model III	model IV
Natural Atomic Charges				
O_1	−0.676	−0.662	−0.672	−0.653
O_2	−0.922	−0.980	−0.952	−0.958
O_3	−0.553	−0.578	−0.568	−0.598
H	0.506	0.509	0.507	0.509
C	0.672	0.697	0.675	0.703
Donor−Acceptor Orbital Stabilization [kcal/mol]				
$LP(O_2) \rightarrow BD^*(O_1-H)$	30.7	31.5	31.9	33.1
$LP(O_1) \rightarrow BD^*(C=O_3)$	50.5	52.8	51.7	54.6
$LP(O_3) \rightarrow BD^*(O_2-H)$	—	8.2	9.0	9.9
Total Stabilization Energy [kcal/mol]				
	10.0	15.1	17.6	45.2
no. of H-bonds	1 SHB	1 SHB + 1 LHB	1 SHB + 1 LHB	2 SHB + 2 LHB

[a]See Figure 3 for graphical presentation.

significantly enhanced polarization of the $C=O_3$ bond that exceeds markedly the separate effects of models II and III.

Examination of the stabilization energies based on the interaction between the occupied (bond or lone pair) and the vacant (antibond) orbitals shows that there exists an electron delocalization pathway from the $O_1—H\cdots O_2$ moiety to the $C=O_3$ bond and further around the ring in the direction opposing the $O_1—H$ and $O_2—H$ bond vectors (Figure 3). The electron delocalization tendency is reflected in the stabilization interaction between the occupied lone pair natural orbitals and the vacant antibond orbitals listed in Table 1. These interactions are computed in the NBO analysis by means of the second order perturbation approach; it should be noted that the calculated values should not be compared with the energies of covalent bonds or H-bonds. The stabilization energies feature a clear trend with the size of the model; in all examples of the addition of molecules to model I, the interaction between the lone pair on O and the O−H antibond is enhanced. Addition of a water molecule close to the $C=O_3$ group and of another oxalic acid molecule (models II and III, respectively) provides a comparable enhancement of the delocalization while in the case of a ring formation (model IV) the cooperative effect is approximately equal or slightly exceeds the sum of both. The NBO results on bond-antibond interactions are similar to the general trends of electronic effects accompanying the strength of H-bonds.

The enhanced delocalization of the lone pair electrons caused by the ring formation is a driving force for the shortening of the $O_1—H\cdots O_2$ hydrogen bond. Namely, delocalization of the lone pairs on O_2 and O_1 into the $O_1—H$ and $C=O_3$ antibond orbitals is in essence equivalent to the weakening of the $O_1—H$ and $C=O_3$ bonds. Therefore, it is plausible for the $O_1—H$ and $C=O_3$ bond distances to lengthen under the influence of the additional water molecules or circular motifs. In virtually all H-bonds the migration of the proton toward the center of the donor−acceptor line is accompanied by the shrinking of the donor−acceptor distance.[62] Hence, by weakening the $O_1—H$ bond the $O_1\cdots O_2$ distance decreases as observed with the optimized 1A2W cluster model (Figure 1a) in which the original O···O distance of 2.71 Å shrinks to 2.65 Å on addition of two water molecules (1A4W cluster, Figure 1b) and also in other clusters with circular motifs (Figure 1c−f) in which the optimized O···O distance of ∼2.6 Å is shorter than in the 1A2W cluster. These findings are in qualitative agreement with the trend found in the NBO study of cooperation in H-bonded HCN clusters, in that the increasing H-bond strength is accompanied with a progressive charge transfer from the lone pair located at the H-bond accepting nitrogen atom into the C−H antibond orbital.[39]

Apart from the trends in the NBO-computed parameters (Table 1) on adding explicit environment to the complex of oxalic acid and water, similar trends are observed in several related quantities. Namely, many other bond−antibond stabilization interactions are changed and the trend in these quantities, though usually smaller, is in full accord with the above presented result that the hydrogen bond surroundings causes a shrinking of the $O_1\cdots O_2$ distance, particularly when arranged in a ring.

The total stabilization energy of the cluster relative to its monomeric constituents (Table 1) is another measure of the cooperative effect. For instance, the counterpoise corrected stabilization energy of model II is 15.1 kcal/mol while for model III it equals 17.6 kcal/mol, corresponding mainly to one SHB and one LHB in both cases. In contrast, model IV contains a double amount of H-bonds, namely two SHB's and two LHB's arranged in a ring, implying a total stabilization energy of about 30−35 kcal/mol in the absence of cooperativity. However, the computed total stabilization energy of model IV is as large as 46.5 kcal/mol, exceeding the double amount of model II and III by at least 11.2 kcal/mol and indicating strong cooperativity. While other nonbonding interactions may also contribute to the stabilization energy, it is highly unlikely that they could cause such a marked increase on forming the ring.

The formation of large clusters of hydrated oxalic acid causes an accumulation of the above presented effects. This is particularly well expressed in the crystal structure in which each C=O group accepts two H-bonds from two distinct water molecules, which is in agreement with the reasoning of Vishweshwar et al.[32] It can be assumed that in the 5A8W cluster (Figure 1g) the $O_1—H\cdots O_2$ H-bonds of the central oxalic acid molecule are notably shorter than in the smaller clusters, which also is in good agreement with the experimental data due to the cumulation of the above-discussed effects.

3.3. Comparison between α- and β-OADH. The two polymoprhs of OADH exhibit subtle differences in the packing pattern. Both polymorphs include topologically similar motifs, and the most pronounced difference related to the SHB is the orientation of the water molecule accepting the SHB from the acid. The alignment of one acid and two water molecules is shown in Figure 4.

While in α-OADH the alignment of the water molecule renders the position of its hydrogen atoms, relative to the acid, notably inequivalent, its alignment in β-OADH almost sustains the approximate C_{2h} symmetry. The O−H group of the acid is nearly coplanar with the water molecule.

The alignment of molecules in α-OADH is apparently more favorable for the formation of the H-bond. Namely, the orientation of the water molecule facilitates the lone pair located at the accepting oxygen atom to be well aligned with the O···H line defining the H-bond. This is much less the case in β-OADH, where the alignment of acid and water prevents the lone pair to be located near the O···H line. Indeed, the computed lone pair Wannier centers confirm this; the offset from the O···H line is much smaller in the α than in the β model (Figure 4).

dx.doi.org/10.1021/ct500167n | J. Chem. Theory Comput. 2014, 10, 1817−1823

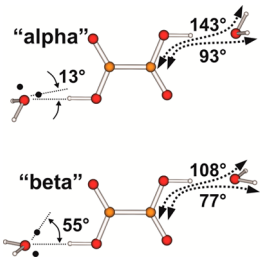

Figure 4. Heterotrimer model representing the α- and β-polymorph of OADH. On the right-hand side, the torsional orientation of the water molecule is displayed as the H−O···O−C dihedral angle of both hydrogen atoms (taken from the experimental crystal structure of the polymorphs). On the left-hand side, the Wannier centers (black dots) representing the lone electron pairs are displayed and their offset from the H-bond direction defined by the O···H line is indicated. Note that the only difference between the α-model and β-model lays in the torsional alignment of the acid and water molecules. All the other internal parameters are the same with both models.

How is this reflected in the H-bond shrinking tendency? The NBO computed lone pair O−H antibond stabilization energy reveals a sizable difference between the α- and β-arrangements, the former yielding notably larger stabilization (Table 2).

Table 2. Comparison of Selected Geometric Parameters (Computed and Experimental), NBO Lone Pair−Antibond Stabilization Energy, H-Bond Energy, and Charge Transfer between the Polymorphs or Their Heterotrimer Models

property	α	β
H−O···O−C torsions (experimental) [deg]	93, 143	77, 108
Offset of LP(O_2) from O···H line [deg]	13	55
NBO: LP(O_2) → BD*(O_1−H) [kcal/mol]	26.1	23.6
H-bond energy [kcal/mol]	6.71	6.57
charge transfer water → acid [electrons]	0.052	0.044
$R_{O\cdots O}$ (calculated, PBC) [Å]	2.49	2.53
$R_{O\cdots O}$ (experimental) [Å]	2.49	2.54

Consequently, the H-bond enhancement is more pronounced in α-OADH, supporting the shorter O···O distance, both measured and calculated. The more favorable geometric arrangement in the α model is also reflected in the higher H-bond energy and larger negative charge transfer from water to acid (Table 2). Similarly to the α-polymorph the periodic calculation reasonably reproduces the structure of the β-polymorph, including the slightly longer O···O distance. While the periodic calculation does not provide insight into factors governing the shortness of the H-bond, the good match between calculation and experiment additionally validates the employed DFT methodology. The quantities demonstrating the difference in H-bonds between the polymorphs are displayed in Table 2.

Having assessed the factors causing the shortness of the H-bond in both α- and β-OADH, we believe that the same reasoning can be applied to related systems featuring similar crystal and electron structures, for example, acetylene dicarboxylic acid dihydrate.[26] It is likely that these systems undergo similar H-bond shortening due to the cooperative effect enhanced by polarization as demonstrated for OADH.

4. CONCLUSIONS

The trends both in the metric and electronic parameters exhibited by the model clusters with increasing the number of participating oxalic acid and water molecules (Figure 1) shows clearly that the cooperative effect is the major factor in the shortening of H-bonds. This is particularly well pronounced in the optimized $R_{O\cdots O}$ of the carboxylic hydroxyl group bonded to the water molecules. One of the most eloquent steps in the reduction of $R_{O\cdots O}$ is between the hydrated single molecule and the circular model consisting of two acid and two water molecules, indicating that it is the circular motif that primarily supports cooperativity. However, both the polarization evoked by the hydration of the carbonyl groups as well as the crystal field effect also contribute notably to the shortening.

NBO analysis of the electron density of the clusters (Figure 2) further reveals the role of circular motifs in the shortening of the SHB by means of cooperativity. The source of H-bond enhancement are the donor−acceptor interactions involving the lone pair and bond orbitals as electron donors and the O−H antibond orbitals as acceptors. Circular structures of alternating acid and water molecules notably enhance these interactions, giving rise to the weakening and elongation of the O−H bonds and, consequently, to the shortening of the O···O distances. Polarization of the involved bonds, particularly the C═O bond, represents a significant part of these effects. Importantly, it appears that the effect of ring formation can exceed the sum of contributions of the individual intermolecular interactions, confirming the existence and relevance of cooperativity. This is particularly pronounced in the total interaction energy.

Additional insight into factors causing the shortness of the H-bond is obtained by comparing the α- and β-polymorph of OADH. The subtle difference in the torsional alignment of the acid and water molecules is reflected in a notable change in the part of the density involved in the H-bond, in that the formation of a short H-bond is more favorable in α-OADH.

■ ASSOCIATED CONTENT

Ⓢ Supporting Information

Experimental infrared spectra demonstrating the relatively modest H-bonding in aqueous and anhydrous oxalic acid and performance comparison between the BLYP, PBE, and B3LYP functionals. This material is available free of charge via the Internet at http://pubs.acs.org.

■ AUTHOR INFORMATION

Corresponding Author

*E-mail: jernej.stare@ki.si.

Notes

The authors declare no competing financial interest.

■ ACKNOWLEDGMENTS

Financial support of the Slovenian Research Agency (program codes P1-0010 and P1-0012) is gratefully acknowledged. We thank Jože Grdadolnik (National Institute of Chemistry) for providing the experimental spectra included in Supporting Information.

■ REFERENCES

(1) Robertson, J. M.; Woodward, I. *J. Chem. Soc.* **1936**, 1817−1824.
(2) Robertson, J. M.; Ubbelohde, A. R. *Proc. R. Soc. A* **1939**, *170*, 222−240.
(3) Brill, R.; Hermann, C.; Peters, C. *Annalen Der Physik* **1943**, *42*, 357−377.
(4) Dunitz, J. D.; Robertson, J. M. *J. Chem. Soc.* **1947**, 142−148.
(5) Ahmed, F. R.; Cruickshank, D. W. J. *Acta Crystallogr.* **1953**, *6*, 385−392.

(6) Delaplane, G.; Ibers, J. A. *Acta Crystallogr., B* **1969**, *B 25*, 2423−2437.
(7) Delaplane, G.; Ibers, J. A. *J. Chem. Phys.* **1966**, *45*, 3451−3452.
(8) Coppens, P.; Sabine, T. M. *Acta Crystallogr., B* **1969**, *B 25*, 2442−2451.
(9) Sabine, T. M.; Cox, G. W.; Craven, B. M. *Acta Crystallogr., B* **1969**, *B 25*, 2437−2441.
(10) Putkonen, M. L.; Feld, R.; Vettier, C.; Lehmann, M. S. *Acta Crystallogr., B* **1985**, *41*, 77−79.
(11) Lehmann, A.; Luger, P.; Lehmann, C. W.; Ibberson, R. M. *Acta Crystallogr., B* **1994**, *50*, 344−348.
(12) Coppens, P.; Sabine, T. M.; Delaplane, G.; Ibers, J. A. *Acta Crystallogr., B* **1969**, *B 25*, 2451−2457.
(13) Stevens, E. D.; Coppens, P. *Acta Crystallogr., B* **1980**, *36*, 1864−1876.
(14) Stevens, E. D.; Coppens, P.; Feld, R.; Lehmann, M. S. *Chem. Phys. Lett.* **1979**, *67*, 541−543.
(15) Coppens, P.; Dam, J.; Harkema, S.; Feil, D.; Feld, R.; Lehmann, M. S.; Goddard, R.; Kruger, C.; Hellner, E.; Johansen, H.; Larsen, F. K.; Koetzle, T. F.; Mcmullan, R. K.; Maslen, E. N.; Stevens, E. D.; Coppens, P. *Acta Crystallogr., A* **1984**, *40*, 184−195.
(16) Dam, J.; Harkema, S.; Feil, D. *Acta Crystallogr B* **1983**, *39*, 760−768.
(17) Wang, Y.; Tsai, C. J.; Liu, W. L.; Calvert, L. D. *Acta Crystallogr., B* **1985**, *41*, 131−135.
(18) Zobel, D.; Luger, P.; Dreissig, W.; Koritsanszky, T. *Acta Crystallogr., B* **1992**, *48*, 837−848.
(19) Martin, A.; Pinkerton, A. A. *Acta Crystallogr., B* **1998**, *54*, 471−477.
(20) Casati, N.; Macchi, P.; Sironi, A. *Chem. Commun.* **2009**, 2679−2681.
(21) Chakoumakos, B. C.; Cao, H. B.; Ye, F.; Stoica, A. D.; Popovici, M.; Sundaram, M.; Zhou, W. D.; Hicks, J. S.; Lynn, G. W.; Riedel, R. A. *J. Appl. Crystallogr.* **2011**, *44*, 655−658.
(22) Feil, D. *J. Mol. Struct.* **1990**, *237*, 33−46.
(23) Krijn, M. P. C. M.; Feil, D. *J. Chem. Phys.* **1988**, *89*, 4199−4208.
(24) Krijn, M. P. C. M.; Graafsma, H.; Feil, D. *Acta Crystallogr., B* **1988**, *44*, 609−616.
(25) Bartashevich, E. V.; Nikulov, D. K.; Vener, M. V.; Tsirelson, V. G. *Comput. Theor. Chem.* **2011**, *973*, 33−39.
(26) Dunitz, J. D.; Robertson, J. M. *J. Chem. Soc.* **1947**, 148−154.
(27) Dunitz, J. D.; Robertson, J. M. *J. Chem. Soc.* **1947**, 1145−1156.
(28) Iwasaki, F. F.; Saito, Y. *Acta Crystallogr.* **1967**, *23*, 56−63.
(29) Macchi, P.; Casati, N.; Marshall, W. G.; Sironi, A. *CrystEngComm* **2010**, *12*, 2596−2603.
(30) Steiner, T. *Angew Chem. Int. Ed.* **2002**, *41*, 48−76.
(31) Vishweshwar, P.; Nangia, A.; Lynch, V. M. *Chem. Commun.* **2001**, 179−180.
(32) Vishweshwar, P.; Babu, N. J.; Nangia, A.; Mason, S. A.; Puschmann, H.; Mondal, R.; Howard, J. A. K. *J. Phys. Chem. A* **2004**, *108*, 9406−9416.
(33) Jeffrey, G. A. *An Introduction to Hydrogen Bonding*; Oxford University Press: New York, 1997.
(34) Hadži, D.; Sheppard, N. T. *Proc. R. Soc. Lond. A* **1953**, *216*, 247−266.
(35) De Villepin, J.; Novak, A.; Bougeard, D. *Chem. Phys.* **1982**, *73*, 291−312.
(36) Derissen, J. L.; Smit, P. H. *Acta Crystallogr., B* **1974**, *30*, 2240−2242.
(37) Mohacek-Grosev, V.; Grdadolnik, J.; Stare, J.; Hadzi, D. *J. Raman Spectrosc.* **2009**, *40*, 1605−1614.
(38) King, B. F.; Farrar, T. C.; Weinhold, F. *J. Chem. Phys.* **1995**, *103*, 348−352.
(39) King, B. F.; Weinhold, F. *J. Chem. Phys.* **1995**, *103*, 333−347.
(40) Kobko, N.; Dannenberg, J. J. *J Phys Chem A* **2003**, *107*, 10389−10395.
(41) Kobko, N.; Paraskevas, L.; del Rio, E.; Dannenberg, J. J. *J. Am. Chem. Soc.* **2001**, *123*, 4348−4349.
(42) Dannenberg, J. J. *J. Mol. Struct.* **2002**, *615*, 219−226.
(43) Del Bene, J. E.; Pople, J. A. *J. Chem. Phys.* **1973**, *58*, 3605−3608.
(44) Ziolkowski, M.; Grabowski, S. J.; Leszczynski, J. *J. Phys. Chem. A* **2006**, *110*, 6514−6521.
(45) Esrafili, M. D.; Fatehi, P.; Solimannejad, M. *Comput. Theor. Chem.* **2013**, *1022*, 115−120.
(46) Adrian-Scotto, M.; Vasilescu, D. *J. Mol. Struct.—Theochem* **2007**, *803*, 45−60.
(47) Znamenskiy, V. S.; Green, M. E. *J. Chem. Theory Comput.* **2007**, *3*, 103−114.
(48) Rossetti, G.; Magistrato, A.; Pastore, A.; Carloni, P. *J. Chem. Theory Comput.* **2010**, *6*, 1777−1782.
(49) Levstik, A.; Filipic, C.; Bobnar, V.; Levstik, I.; Hadzi, D. *Phys. Rev. B* **2006**, *74*, 153104.
(50) Birczynski, A.; Sulek, Z.; Muller, A.; Haeberlen, U. *Z. Phys. Chem.* **1992**, *178*, 133−155.
(51) Sagnowski, S.; Aravamudhan, S.; Haeberlen, U. *J. Chem. Phys.* **1977**, *66*, 4697−4698.
(52) Zhang, Q. W.; Chekmenev, E. Y.; Wittebort, R. J. *J. Am. Chem. Soc.* **2003**, *125*, 9140−9146.
(53) King, M. D.; Korter, T. M. *J. Phys. Chem. A* **2010**, *114*, 7127−7138.
(54) Tomasi, J.; Mennucci, B.; Cammi, R. *Chem. Rev.* **2005**, *105*, 2999−3093.
(55) Frisch, M. J.; Trucks, G. W.; Schlegel, H. B.; Scuseria, G. E.; Robb, M. A.; Cheeseman, J. R.; Scalmani, G.; Barone, V.; Mennucci, B.; ; Petersson, G. A.; Nakatsuji, H.; Caricato, M.; Li, X.; Hratchian, H. P.; Izmaylov, A. F.; Bloino, J.; Zheng, G.; Sonnenberg, J. L.; Hada, M.; Ehara, M.; Toyota, K.; Fukuda, R.; Hasegawa, J.; Ishida, M.; Nakajima, T.; Honda, Y.; Kitao, O.; Nakai, H.; Vreven, T.; J. A. Montgomery, J.; Peralta, J. E.; Ogliaro, F.; Bearpark, M.; Heyd, J. J.; Brothers, E.; Kudin, K. N.; Staroverov, V. N.; Kobayashi, R.; Normand, J.; Raghavachari, K.; Rendell, A.; Burant, J. C.; Iyengar, S. S.; Tomasi, J.; Cossi, M.; Rega, N.; Millam, J. M.; Klene, M.; Knox, J. E.; Cross, J. B.; Bakken, V.; Adamo, C.; Jaramillo, J.; Gomperts, R.; Stratmann, R. E.; Yazyev, O.; Austin, A. J.; Cammi, R.; Pomelli, C.; Ochterski, J. W.; Martin, R. L.; Morokuma, K.; Zakrzewski, V. G.; Voth, G. A.; Salvador, P.; Dannenberg, J. J.; Dapprich, S.; Daniels, A. D.; Farkas, O.; Foresman, J. B.; Ortiz, J. V.; Cioslowski, J.; Fox, D. J. *Gaussian 09*, Revision A.02; Gaussian, Inc.: Wallingford, CT, 2009.
(56) *CPMD V3.13*, Copyright IBM Corp 1990−2008, Copyright MPI fuer Festkoerperforschung Stuttgart 1997−2001.
(57) Troullier, N.; Martins, J. L. *Phys. Rev. B* **1991**, *43*, 1993−2006.
(58) Monkhorst, H. J.; Pack, J. D. *Phys. Rev. B* **1976**, *13*, 5188−5192.
(59) Reed, A. E.; Curtiss, L. A.; Weinhold, F. *Chem. Rev.* **1988**, *88*, 899−926.
(60) Wannier, G. H. *Phys. Rev.* **1937**, *52*, 191−197.
(61) Marzari, N.; Mostofi, A. A.; Yates, J. R.; Souza, I.; Vanderbilt, D. *Rev. Mod. Phys.* **2012**, *84*, 1419−1475.
(62) Novak, A. *Struct. Bonding (Berlin)* **1974**, *18*, 177−216.